FEM-BASED DESIGN OF HOLLOW SECTIONS AGAINST LOCAL, GLOBAL AND INTERACTIVE BUCKLING – MODEL VERIFICATION AND CALIBRATION AGAINST PHYSICAL TESTS

ANDREA TOFFOLON[1], IGOR NIKO[2] and ANDREAS TARAS[3]

[1]Bundeswehr University Munich, Department of Civil Engineering, Werner-Heisenberg-Weg 39, 85579, Neubiberg, Germany .
E-mail: andrea.toffolon@unibw.de
[2] Slovak University of Technology, Department of Steel and Timber Structures, Radlinského 11, 810 05, BratislavaSlovakia
[3]ETH Zurich, Institute of Structural Engineering, Chair of Steel and Composite Structures, Stefano-Franscini-Platz, 8093 Zürich.
E-mail: taras@ibk.baug.ethz.ch

Inadequate knowledge regarding specific local and interactive behavior of slender hollow sections made of both mild steel and high-strength steel (HSS) presents an obstacle for the more wide-spread introduction of these sections in the construction practice. Current design approaches are simplified and often yield overtly conservative results. Dealing with non-standard cross-sections only exacerbates these difficulties. Within the EU-funded project "HOLLOSSTAB, which is concerned with improving the afore-mentioned situation, advanced shell-element FEM models were verified, validated and calibrated against a very large series of physical tests. Thereby, new knowledge was obtained regarding the modelling of instability effects stemming from geometrical imperfections, residual stresses and non-linear material constitutive laws. This paper gives an overview of the experimental test campaign of HOLLOSSTAB and of the developed FEM models for Geometrically and Materially Non-Linear Analyses with Imperfections (GMNIA). The test data thereby comprise RHS, SHS, CHS, hexagonal and other non-standard cross sections, and the steel grade ranges from S355 to S890. The developed verified and validated models may be used for research and development projects, as well as design projects that allow for the use of advanced FEM-based design. The state-of-the-art measuring tools used in the project offer the possibility of carrying out a precise reverse-engineering process, creating a numerical model of experimental test that includes the actual geometry with very high accuracy. The development of buckling deformations was also accurately monitored, using image correlation (DIC) techniques.

Keywords: local buckling; overall buckling resistance; hollow sections; GSRM; high-strength-steel.

1 Introduction

An increasing demand for light-weight, high-performance structures recently expanded the field of application of hollow sections and high-strength steel (HSS). However, current design standards, such as Eurocode 3, do not sufficiently address the resistance of such sections – as well as more common square and rectangular hollow sections - against local (L) and groove-stiffened = "distortional" (D) buckling modes, especially for general combinations of loading (compression

Proceedings of the 17th International Symposium on Tubular Structures.
Editors: X.D. Qian and Y.S. Choo

Published by Research Publishing, Singapore.
ISBN: 978-981-11-0745-0; doi:10.3850/978-981-11-0745-0_094-cd

and mono- or biaxial bending). The EU-funded RFCS-project "HOLLOSSTAB" (2016-2019) set out to eliminate these shortcomings. In this project, cold-formed sections with and without plate grooves, hot-finished and cold-formed circular hollow sections, as well as hexagonal hollow sections made of both mild and high strength steel, were tested in pure compression, bending and bending with compression, with various slenderness ranges for local buckling. This paper illustrates some aspects of HOLLOSSTAB, specifically the validation of advanced FEM models against the project's large experimental campaign, with the aim of applying the FEM model for extensive numerical parametric studies. Finally, the results of the parametric study were used for the development of appropriate design rules for these sections, with a continuous representation of strength throughout slenderness ranges, using the "Generalised Slenderness-based Resistance Method" (GSRM - see Toffolon and Taras, 2019) as a conceptual basis for the development of specific design rules. This concept – in an expansion and focalization on hollow sections of the Direct Strength Method (DSM) used in North America for the design of cold-formed steel open cross-sections – makes use of the results of (numerical) linear buckling analyses (LBA) for the overall section and member to determine the slenderness and consequently an "overall" buckling reduction factor.

2 Scope and Methodology

Six types of cross-sections are the subject of the present study and of the HOLLOSSTAB project. Figure **1** shows the tested cross-sections. In d) and e) rectangular hollow sections (RHS) and square hollow sections (SHS) are represented, in a) SHS with groove stiffeners and in b) T-shape hollow secions with groove stiffeners (respectively referred as SHS-S and SHS-T in the present paper); finally, in c) a hexagonal cross-section and a circular hollow section in f) are shown.

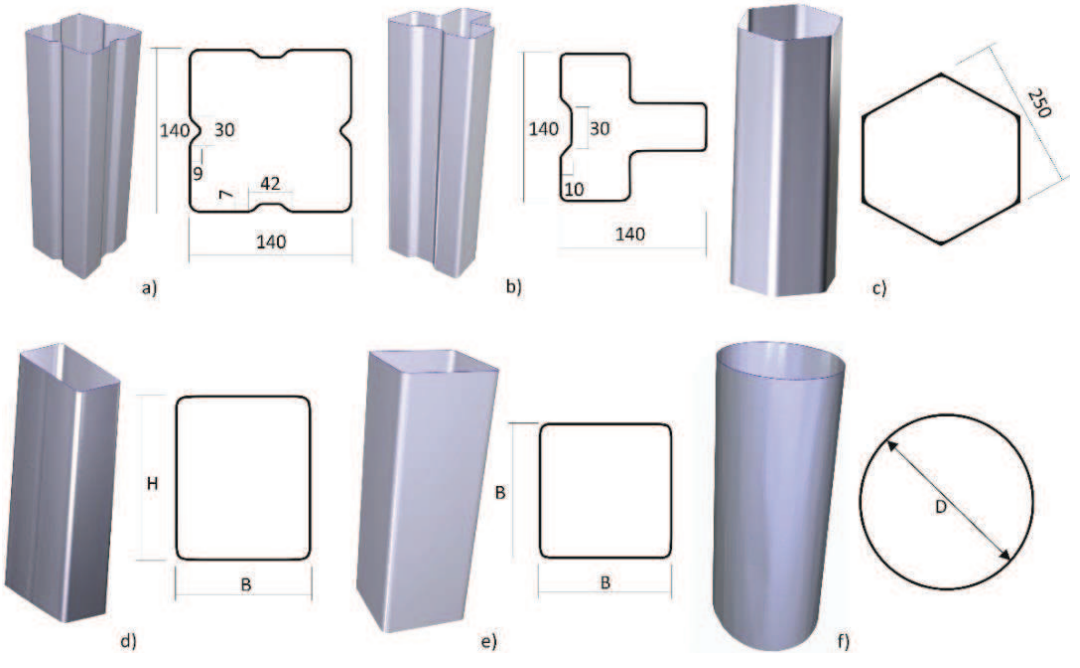

Figure 1. Overview of the test cross-sections with steel grades from (normal strength) S355 to (high strength) S700.

In order to evaluate the effects of different load combinations of N+M on local, distortional and global buckling, different eccentricities and specimen lengths were analysed, In total 55 experimental tests on plated cross-sections and 23 experimental tests on CHS were carried out at the laboratory of Bundeswehr University Munich, see Table 1. The remainder of this section of the paper describes the scope and methodology of the test series.

Table 1. Overview of the test type and corresponding test parameters

Test denomination -	Top eccentricity [mm]	Bottom eccentricity [mm]	Length [mm]
T1	0	0	800
T2	9 – 64	0	800
T3	57 – 196	= top	800
T4	232 - 457	= top	800
T5	57 – 196	= top	2000

2.1 *Local geometric imperfection analysis*

Hollow section manufacturing introduces geometric imperfections, e.g. in cold-formed sections by bending the steel coils and welding the cross-section parts into the final shape. An additional source of imperfections is the preparation of the specimens by cutting and welding the steel tubes for the experimental test. This can significantly influence the structural responses including the onset of buckling, initiation of plasticity and ultimate load-carrying capacity. For this reason, a 3D scanning technique was employed to measure the distribution of local geometric imperfections in each test specimen. After cleaning, the outer surface of the specimens was then scanned using a Zeiss 3D scanner and recorded as point clouds (Figure 1 a). Then, 3D spline curves were laid over the point cloud, in order to be imported into the numerical simulation (Figure 1 b). In Figure 1 c), an example of an evaluation of the measured imperfection against the ideal geometry in 3D. The represented imperfections are located in 2 exemplary cross-sections of an SHS specimen (Figure 1 d), and maximum and minimum value of the imperfection for each cross-section side are shown.

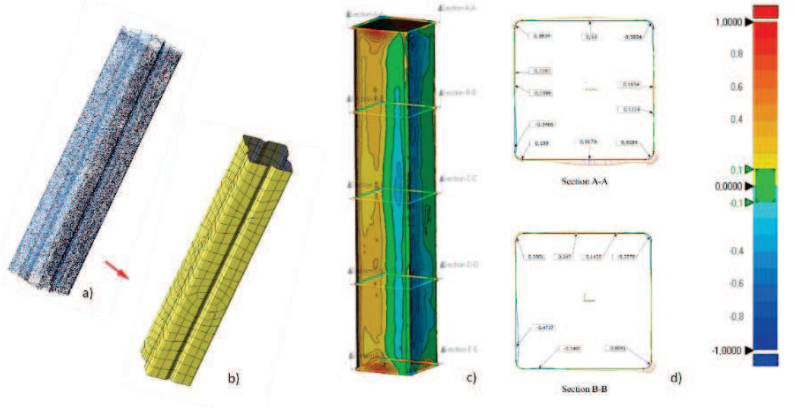

Figure 2. a) point cloud and splines b) of the 3D scan data for a SHS-S; c) 3D imperfection evaluation and d) 2 exemplary cross-section for a SHS.

2.2 *Methodology of the experimental test*

Stub-column tests (with pure compression) and short beam-column tests with different levels of eccentricity were performed to investigate the local buckling behaviour of cross-sections under the N+M load case, as well as global buckling of longer beam-columns. The tests were conducted on a 10 MN servo-hydraulic test rig built by MFL. The test execution was displacement controlled, with a given total displacement (accounting for setup stiffness) ranging from about 10 mm to 100 mm. A constant slow rate test velocity was applied in order to simulate a static problem. The velocity varied between 0.01 mm/s to 0.06 mm/s, and the DIC recording rate was set to 1 Hz, thus providing around 1000 pictures and measurements for each specimen. Figure 3. a) shows a schematic representation of the test setup for pure compression. The actuator transfers the vertical force from the top through the load cell and through the adapter into the test specimen. The load cells incorporate a linear variable displacement transducer (LVDT), with both values directly serving as input in the data acquisition and analysis software. A speckle pattern for the DIC was drawn on the specimen surface, in an area that is visible to both DIC cameras. Figure 3 d) shows the setup for N+M test. Two high strength axisymmetric adapters (Figure 3 b) direct the vertical forces into the axisymmetric pin joint connection - which consists of a spherical bearing – and to the bottom plate. The spherical bearing allows all rotational degrees of freedom, up to max +- 9°, and integrates reference points for the DIC measurement system.

In Table 2., an overview of the results on stub columns tests is given, where the average prediction error was only 1.1%. For a more detailed review of the experimental test results, please refer to the result data in Toffolon and Taras (2019) and Toffolon et al. (2019).

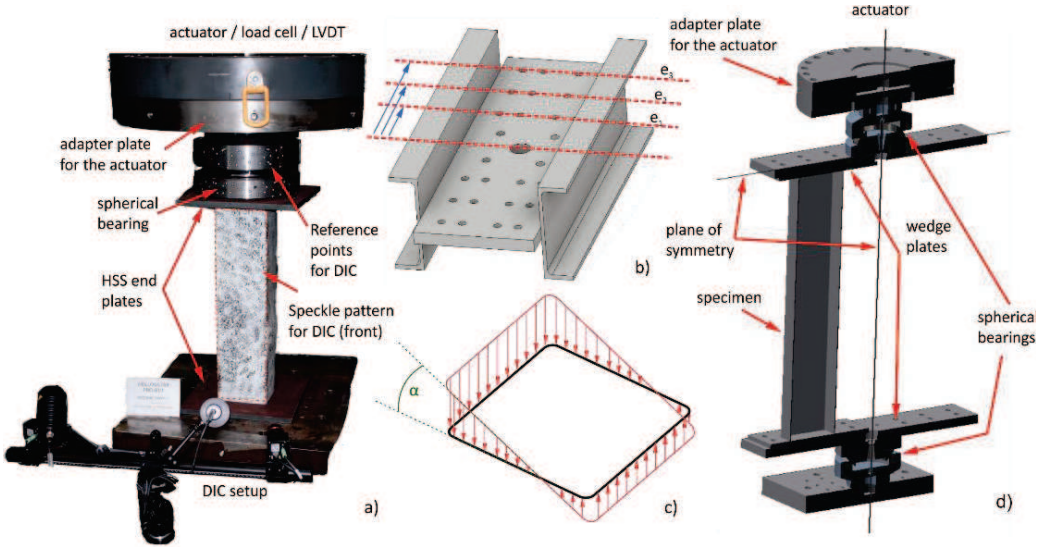

Figure 3. a) testing setup for the T1 and T2 tests b) axisymmetric adapters used for the eccentric T3-T5 tests c) distribution of load on a cross section in eccentric tests d) testing setup for T3-T5 tests.

Table 2. Results of the stub-column tests.

Cross-section -	Grade -	Specimen ID -	Nu,Exp [kN]	Nu,Exp / Nu,FEM -
SHS 140×140×4	S355	T1-1	861.3	0.950
SHS 200×200×5	S355	T1-2	1227.9	0.943
SHS 200×200×8	S355	T1-3	2917.9	0.967
SHS 200×200×4	S500	T1-4	1111.2	0.971
SHS 200×200×5	S500	T1-5	1736.1	0.977
RHS 300×150×6	S355	T1-6	1582.0	0.962
RHS 300×150×8	S355	T1-7	2806.8	1.001
SHS-S 140×140×2.5	S350GD	T1-8	623.1	0.988
SHS-S 140×140×3.5	S350GD	T1-9	1002.4	1.050
HEX250×8.5	S355	T1-10	2925.8	1.018
SHS-T 140×140×2.5	HX460	T1-11	584.5	0.993
SHS-T 140×140×4.0	HX460	T1-12	1098.1	1.034

3 Validation of the Numerical Model

The first step of the validation of a FEM model to be used in larger parametric studies consists in the determination of the mesh density, element type and boundary conditions that best describes the experimental test, provided that measured material and geometry values are used – this type of model is termed GMNIA-MEAS. In the next (main) step, a simpler, more generalized model is developed and calibrated (GMNIA), with a simplified definition of the material model and the geometrical imperfections, yet the same FEM mesh size and element types as the ones validated through the calibration to the experimental tests. The main simplification thus consists in the determination of an equivalent imperfection shape. In the study presented in this paper, the imperfect geometry was derived from the first buckling mode of a Linear Buckling Analysis (LBA), with the amplitude for the buckling waves calibrated as described in section 4.

The proprietary software Simulia ABAQUS was used for all numerical simulations, with linear isoparametric shell elements with reduced integration (element type S4R). As a result of the model calibration, it was found that a mesh density with a minimum of 60 elements in circumferential and 200 elements in longitudinal direction was found to lead to converging results of high accuracy. An example of a FEM model validation is shown in Figure 4. The SHS specimen deformed shape in b) was caused by an eccentric compressive load and the deformations were measuered by the DIC system.

The corresponding GMNIA-MEAS model in a) produces fairly accurate results. In c) and d) a more complex model is shown. Here the pin connection that is modeling the spherical bearing is substituted by a surface interaction between the upper and lower part of the spherical bearing. This model was introduced when more accurate results were necessary. In summary, with the chosen FEM modelling technique and discretization, GMNIA-MEAS model are able to approximate the resulting maximum force of the experimental test with an average error of less than 5% in terms of ultimate load. In most observed cases, the deformation curve follows the test curve very closely.

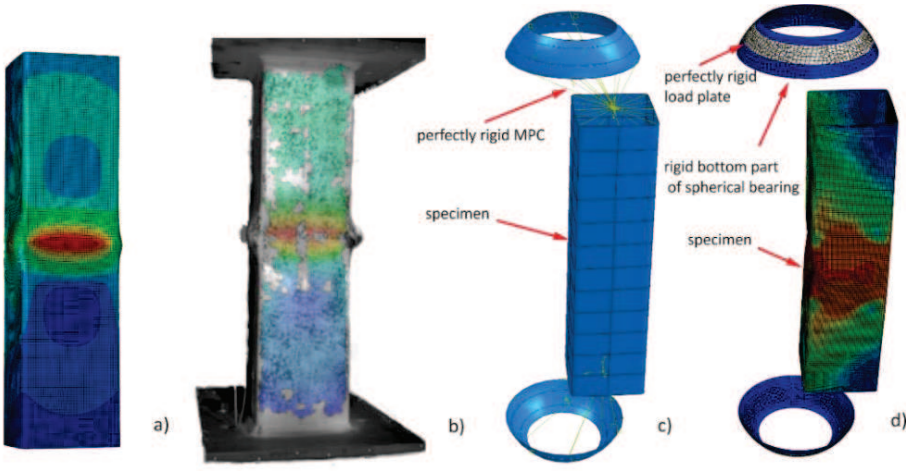

Figure 4. a) GMNIA-MEAS model, b) specimen deformed shape measured with DIC, c) and d) GMNIA-MEAS model with contact.

4 Calibration of the Equivalent Imperfections

In the example of Figure 4., the imperfect geometry was derived from the real geometry, and a GMNIA-MEAS model was thus built and validated. In order to be able to perform a large parametric study that may be used for the calibration of GSRM design rules, an equivalent geometric imperfection with a calibrated imperfection needs to be used. The first buckling mode of a Linear Buckling Analysis (LBA) represents a sensible basis (Boissonnade et al., 2017).

This section investigates the possible values for calibrated imperfection amplitudes for both local and global imperfections that lead to GMNIA parametric study results with sufficient accuracy and conservatism. An LBA modal shape with a calibrated imperfection amplitude is chosen as input for the imperfection calibration for the GMNIA, as well as a standardized strain-stress relation for hot-rolled and cold-formed profiles proposed by Gardner and Yun (2017, 2018).

The GMNIA-MEAS load-deformation curve is first compared to different GMNIA calculations with varying equivalent imperfection amplitude for local buckling in Figure 5. The imperfection amplitudes in this figure range from B/400 up to B/200, where B is the largest cross-section part subjected to compression. Another sample of parametric studies for the case of RHS and local buckling is given in Figure 6.

For the calibration of the numerical model for the global analysis a different approach was chosen. Similarly to the local buckling, the equivalent imperfection shape derive from the first non-global eigenmode of a LBA analysis. The difference lies in the comparison basis for the calibration of the imperfection amplitude. A comparison with the well-established buckling curve “a” (for hot-rolled sections) and “c” (for cold-formed sections) from EC3-1-1 and imperfection values from the literature was made, and the results are shown in the following. An imperfection amplitude of L/850 most closely matches the EC3 curves, with the value of L/1000 often cited in the literature (see e.g. Gardner, 2017; Taras, 2016)leading to almost identical results. The latter was thus chosen for the further parametric study. In Figure 7., the results of the calibration for global buckling are represented for hot-finished cross-sections and cold-formed cross-sections.

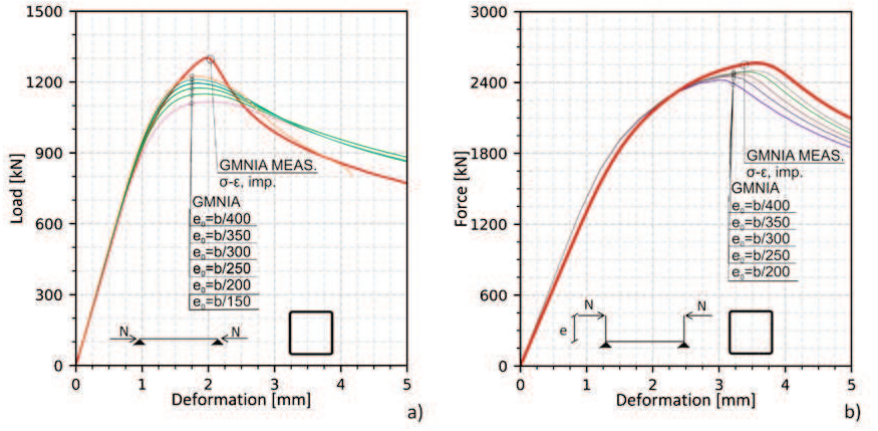

Figure 5. Calibration of the imperfection amplitude for a a) SHS 200×200×5 S355 (T1), and b) SHS 200×200×8 S355 (T2)

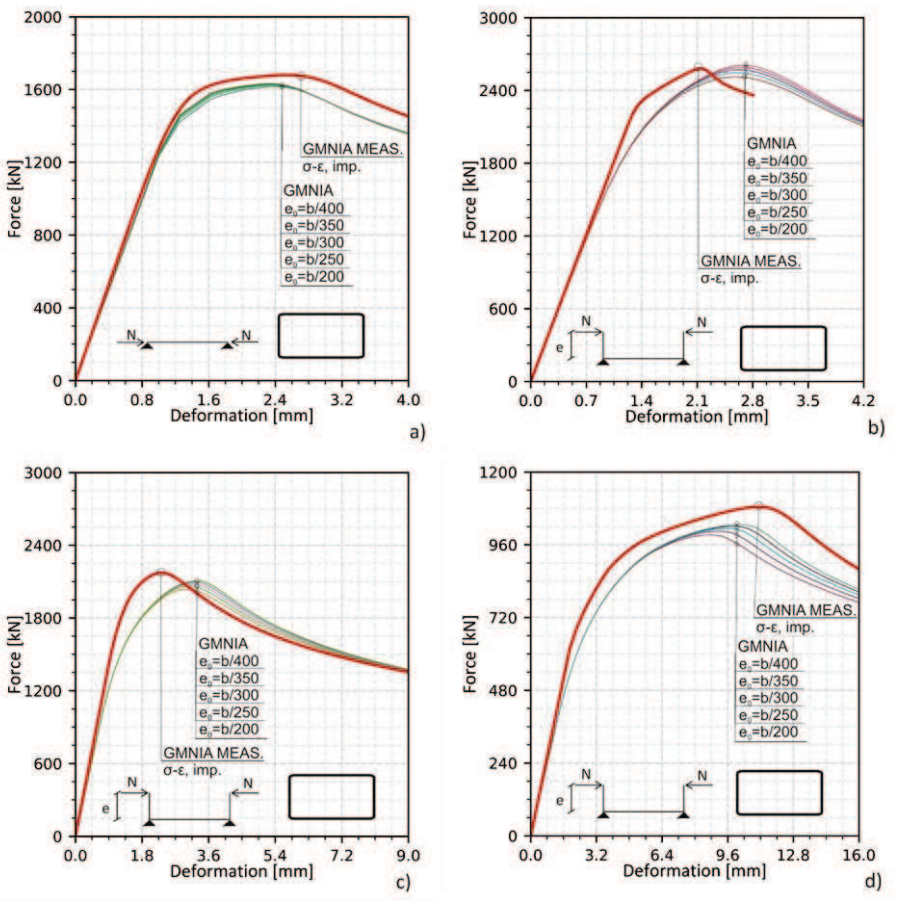

Figure 6. Calibration of the imperfection amplitude for a a) stub column test (T1) RHS 300×150×8 S355, and for the beam column tests b) RHS 300×150×8 S355 (T2), c) RHS 300×150×8 S355 (T3) and d) RHS 300×150×8 S355 (T4).

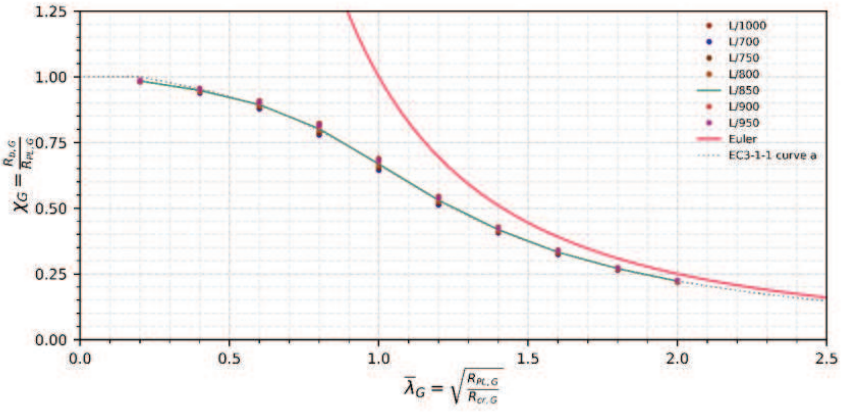

a)

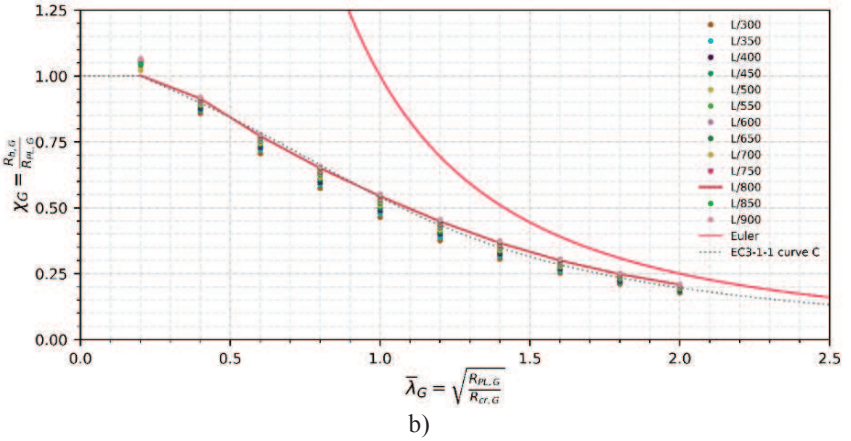

b)

Figure 7. Calibration of the imperfection for global buckling model. In a) the results for the hot-rolled EN10210 cross-sections are shown, and similarly for cold-formed according to EN10219 in b).

5 Summary and Conclusions

This paper discussed work carried out within the European research project HOLLOSSTAB, during which new design rules for hollow sections with innovative shapes and/or steel grades are developed on the basis of the new "Generalised Slenderness-based Resistance Method" (GSRM).

The focus of the paper was put on the validation and calibration of the GMNIA model for extensive numerical campaigns that formed the basis for the validation and calibration of GSRM design rules. The latter are shown in a separate paper by the authors at this conference and – in full detail – in Taras et al. (2019a).

Acknowledgments

The authors would like to acknowledge the funding received by the European Community's Research Fund for Coal and Steel (RFCS) under grant agreement No. 709892 - HOLLOSSTAB.